Pis'ma v ZhETF, vol. 88, iss. 2, pp. 115 – 118

Electronic structure of new oxygen-free 38 K superconductor $Ba_{1-x}K_xFe_2As_2$ in comparison with $BaFe_2As_2$ from first principles

I. R. Shein, A. L. Ivanovskii*

Institute of Solid State Chemistry, Ural Branch RAS, 620041 Ekaterinburg, Russia

Submitted 6 June 2008

Based on first-principles FLAPW-GGA calculations, we have investigated the electronic structure of the newly discovered oxygen-free 38 K superconductor $Ba_{1-x}K_xFe_2As_2$ in comparison with a parent phase – the tetragonal ternary iron arsenide $BaFe_2As_2$. The density of states, magnetic properties, near-Fermi bands compositions, together with Sommerfeld coefficients γ and molar Pauli paramagnetic susceptibility χ have been evaluated. The results obtained allow us to classify these systems as *quasi-two-dimensional ionic metals*, where conduction is strongly anisotropic, happening only in the (Fe-As) layers. According to our calculations, in the case of hole doping of $BaFe_2As_2$, the density of states at the Fermi level grows, which, possibly, may be a factor promoting the occurrence of superconductivity for $Ba_{1-x}K_xFe_2As_2$. On the other hand, $Ba_{1-x}K_xFe_2As_2$ lies at the border of magnetic instability and pairing interactions might involve magnetic or orbital fluctuations.

PACS: 71.15.Mb, 71.18.+y, 74.25.Jb

Since the discovery (in February 2008 [1]) of superconductivity with $T_C \sim 26$ K in the fluorine-doped quaternary La-Fe oxyarsenide $LaO_{1-x}F_xFeAs$, further promising developments [2, 3] in search for related oxypnictide-based superconductors (SCs) have been achieved, in particular with replacing La atoms by other rare-earth metals (Ln = Gd [4], Ce [5], Sm [6], Pr and Nd [7, 8]), resulting in $T_C \sim 41-55$ K. Moreover, comparable values of T_C have been reported for replacing of rare-earth atoms by Th ($Gd_{1-x}Th_xOFeAs$) [9] or Sr ($La_{1-x}Sr_xOFeAs$, where $x \sim 0.09-0.20$) [10], as well as for undoped oxygen-deficient samples $LnO_{1-\delta}FeAs$ (Ln = Sm, Nd, Pr, Ce, La) [11].

These unusual materials attract now considerable interest because they are the first non-Cu-based layered superconductors adopting a comparably high critical temperature and the upper critical field, are located on the border of magnetic instability, and should have an unconventional mechanism of superconductivity, which may be connected with magnetic fluctuations and a spin density wave (SDW) anomaly.

The parent phase – oxyarsenide LaOFeAs adopts the tetragonal ZrCuSiAs-type structure (space group $P4/nmm$) [12], where positively charged $(La\text{-}O)^+$ layers alternate with negatively charged $(Fe\text{-}As)^-$ layers along the c axis; the bonding between these layers is mostly ionic. On the other hand, though the chemical bonding in the (La-O) layers is also ionic, strong covalent interactions occur inside the (Fe-As) layers. According to the available experimental and theoretical data [13 – 19] for LaOFeAs, the electronic bands in a window around the Fermi level are formed mainly by the states of the (Fe-As) layers, whereas the bands of the (La-O) layers are rather far from the Fermi level. Thus, superconductivity in LaFeAsO is determined mainly by structural and electronic states of the (Fe-As) layers.

Recently, a related system – the ternary iron arsenide $BaFe_2As_2$ was investigated and a SDW anomaly similar to that in LaFeAsO was found at 140 K [20]. Moreover, this phase with a tetragonal $ThCr_2Si_2$-type structure (space group $I4/mmm$) [21] contains identical (Fe-As) layers formed of $[FeAs_4]$ tetrahedra, which are separated by barium sheets instead of (La-O) layers in LaFeAsO. In both phases, one electron is transferred to the (Fe-As) layer according to the ionic picture: $Ba^{2+} \rightarrow 0.5(FeAs)^-$ and $(LaO)^+ \rightarrow (FeAs)^-$. The authors of [20] assumed that $BaFe_2As_2$ may be a suitable parent phase in the search for a new family of oxygen-free SCs. Really, quite recently [22] a superconducting transition at $T_C \sim 3$ K was observed for $BaNi_2P_2$, which belongs to the same $ThCr_2Si_2$-like structural type. Moreover, it was found [23] that the ternary iron arsenide $BaFe_2As_2$ with partial substitution $K \rightarrow Ba$ becomes superconducting to $T_C \sim 38$ K for $Ba_{0.6}K_{0.4}Fe_2As_2$.

In these Communications we present the first results of the *ab initio* calculations of the electronic properties for the above mentioned iron arsenide systems, namely, the newly discovered 38 K oxygen-free superconductor $Ba_{1-x}K_xFe_2As_2$ in comparison with a parent phase – the tetragonal ternary iron arsenide $BaFe_2As_2$.

The positions of the atoms for the tetragonal arsenide $BaFe_2As_2$ are: Ba at $2a$ $(0, 0, 0)$, Fe at $4d$ $(0.5, 0, 0.25)$ and As at $4c$ $(0, 0, z)$. To explore the superconducting phase, one barium atom in the double $(a \times a \times c)$ unit

cell of $BaFe_2As_2$ was replaced by a K atom to simulate a hole-doped system with the nominal composition $Ba_{0.5}K_{0.5}Fe_2As_2$ and space group $Cmmm$, see Fig.1.

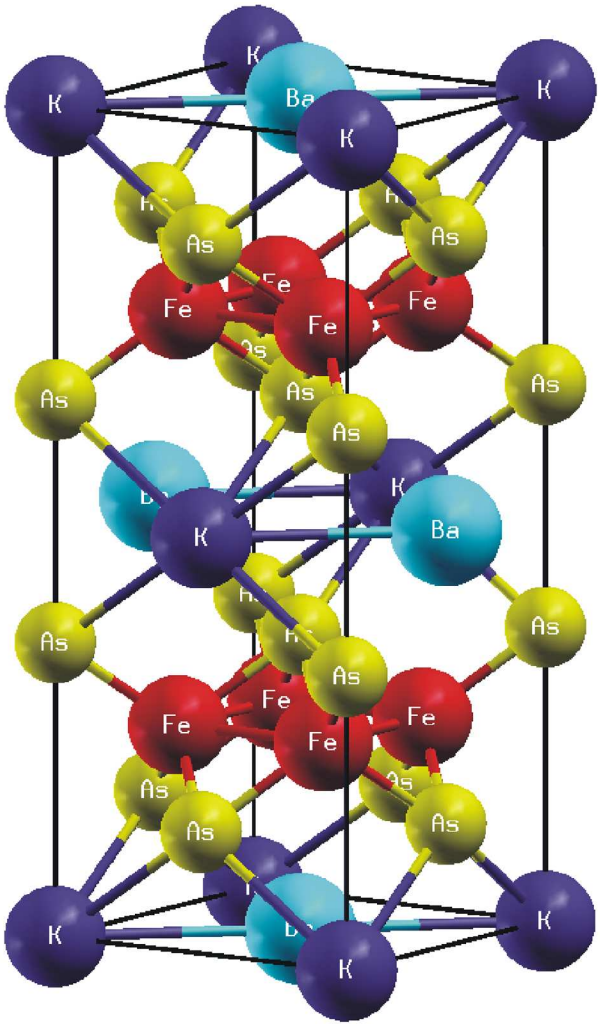

Fig.1. Crystal structure of the ordered phase $Ba_{0.5}K_{0.5}Fe_2As_2$

Our band-structure calculations were carried out by means of the full-potential method with mixed basis APW+lo (LAPW) implemented in the WIEN2k suite of programs [24]. The generalized gradient correction (GGA) to exchange-correlation potential in the PBE form [25] was applied. The experimentally determined lattice parameters and internal positions z for $BaFe_2As_2$ and $Ba_{0.5}K_{0.5}Fe_2As_2$ (listed in Table 1) were used. Two series of calculations were performed: for the nonmagnetic (NM) and magnetic states – in the approximation of FM ordering.

The difference in the energy of magnetic and nonmagnetic states for LaOFeAs and $BaFe_2As_2$ is very small and does not exceed ~ 0.076 eV/form.unit for $BaFe_2As_2$ and ~ 0.046 eV/form.unit for $Ba_{0.5}K_{0.5}Fe_2As_2$, i.e. these materials lie at the border of their magnetic instability.

Table 1

The lattice parameters (a and c, in Å), internal coordinates (z), some interatomic distances (d, in Å) and bond angles As-Fe-As (in deg.) for $BaFe_2As_2$ and $Ba_{1-x}K_xFe_2As_2$ [20, 23]

Phase/parameter	a	c	z	d(Ba-As)
$BaFe_2As_2$	3.9625	13.0168	0.3538	3.382
$Ba_{1-x}K_xFe_2As_2$	3.9090	13.2122	0.3538	3.372
phase/parameter	d(Fe-As)	d(Fe-Fe)	bond angles	
$BaFe_2As_2$	2.403	2.802	111.1×2; 108.7×4	
$Ba_{1-x}K_xFe_2As_2$	2.396	2.770	109.9	

Let us discuss the main peculiarities of the electronic structure of $BaFe_2As_2$ versus $Ba_{0.5}K_{0.5}Fe_2As_2$ using paramagnetic densities of states (DOSs) as depicted in Fig.2.

For $BaFe_2As_2$, at high binding energies the quasi-core DOSs peaks are located from -14.3 eV to -12.9 eV with the Ba $5p$ states and from -12.0 eV to -10.2 eV with the As $4s$ states, as well as with some admixtures of the Fe $3d$ and Ba $5p$ states. The valence band (VB) extends from -5.4 eV up to the Fermi level $E_F = 0$ eV and includes three main subbands A-C, Fig.2. Among them the first subband A ranging from the VB bottom to -3.8 eV is formed predominantly of comparable contributions of the As $4p$ and Fe $3d$ states. The next subband B (in the region from -3.8 eV to -2.1 eV) contains the main contributions from the Fe $3d$ states, together with an admixture from the As $4p$ states. Thus, the above mentioned subbands A and B are derived from the Fe $3d$ states hybridized with the As $4p$ states and are responsible for covalent Fe-As bonding. Finally, the top of the VB (subband C, in the interval from -2.1 eV to E_F) is derived basically from the Fe $3d$ states. This Fe $3d$-like band intersects the Fermi level and continues to $+2.0$ eV (unoccupied subband D); i.e. the near-Fermi region for $BaFe_2As_2$ is composed mainly of iron states with very small admixtures of As states.

Besides, it is noteworthy that the contributions from the valence states of barium to the occupied subbands A-C andthe bottom of the conduction subband D are negligible, i.e. in $BaFe_2As_2$ these atoms are in the form of cations Ba^{2+}. This means that the Ba sheets and the (Fe-As) layers are linked exclusively by ionic interactions, as distinct from the quaternary oxyarsenide LaOFeAs, where covalent bonding arises between the (La-O) and (Fe-As) layers owing to partial overlapping of the La and As states, see for example [15–18]. Thus,

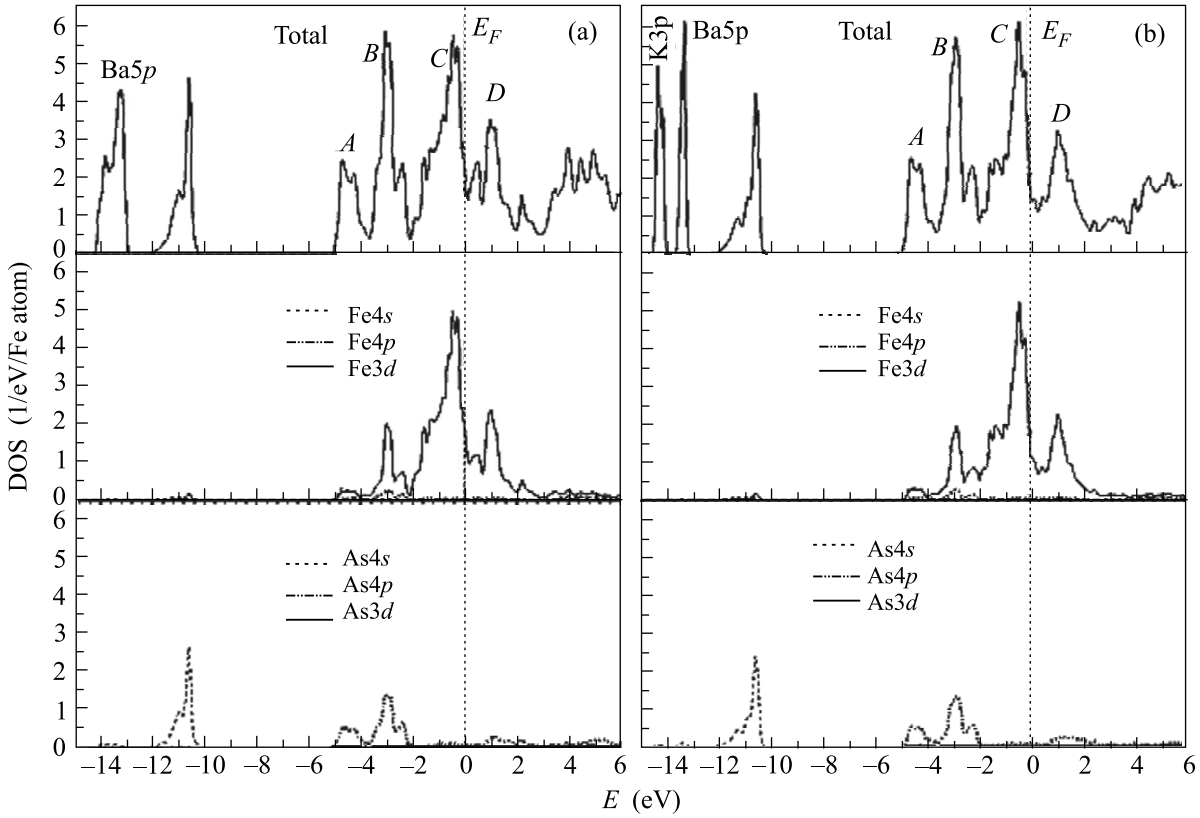

Fig.2. Total and partial densities of states for $BaFe_2As_2$ (a) and $Ba_{0.5}K_{0.5}Fe_2As_2$ (b)

our results indicate that the iron arsenide $BaFe_2As_2$ consists of alternately stacked insulating Ba^{2+} sheets and conductive $(Fe\text{-}As)^{1-}$ layers, and the bonding between them is of the ionic type, i.e. this system may be described as a *quasi-two-dimensional ionic metal*, where conduction is strongly anisotropic, happening only on the (Fe-As) layers.

In turn, the overall shape of the valence DOS for $BaFe_2As_2$ is very similar to that of the potassium doped system, except a new sharp quasi-core peak near -14.3 eV which is derived from K $3p$ states and narrowing of the Ba $5p$ peak, see Fig.2. In both compounds, the valence band which extends from -5.4 eV to the Fermi level (for $BaFe_2As_2$) and from -4.9 to E_F (for $Ba_{0.5}K_{0.5}Fe_2As_2$) is derived basically from the Fe $3d$ states hybridized at the bottom of the VB with the As $4p$ states; some distinctions in DOSs profiles between $BaFe_2As_2$ and $Ba_{0.5}K_{0.5}Fe_2As_2$ (see Fig.2) are related with the deformations of $[FeAs_4]$ tetrahedra building the (Fe-As) layers – as a result of partial replacement of barium by potassium, Table 1. In addition, for $Ba_{0.5}K_{0.5}Fe_2As_2$ the admixtures of Ba and K states in the VB are absent, i.e. this system remains a *quasi-two-dimensional ionic metal.*

The most remarkable difference in the DOS for $BaFe_2As_2$ *versus* $Ba_{0.5}K_{0.5}Fe_2As_2$ is the location of the Fermi level, see Fig.2. For the hole-doped $Ba_{0.5}K_{0.5}Fe_2As_2$, a decrease in the band filling leads to movement of the Fermi level in the region of higher binding energies. As a result, E_F in $Ba_{0.5}K_{0.5}Fe_2As_2$ is shifted downwards and is located on a slope of the sharp peak C in the region of enhanced DOS. Thus, the total density of states at the Fermi level $N(E_F)$ for $Ba_{0.5}K_{0.5}Fe_2As_2$ becomes almost 20% higher than the value of $N(E_F)$ for $BaFe_2As_2$, Table 2. Note that the growth of $N(E_F)$ is achieved exclusively due to the Fe $3d$ states, whereas the contribution from the As states remains less than 4%, Table 2.

Table 2

Total $N^{tot}(E_F)$ and partial $N^l(E_F)$ densities of states at the Fermi level (in states/eV·form.unit), electronic heat capacity γ (in mJ·K^{-2}·mol^{-1}) and molar Pauli paramagnetic susceptibility γ (in 10^{-4} emu/mol) for $BaFe_2As_2$ and $Ba_{0.5}K_{0.5}Fe2As_2$

Phase/parameter	$N^{Fe d}(E_F)$	$N^{As}(E_F)$	$N^{tot}(E_F)$	γ	χ
$BaFe_2As_2$	1.860	0.071	4.553	10.73	1.47
$Ba_{0.5}K_{0.5}Fe_2As_2$	2.352	0.072	5.526	13.03	1.79

These data allow us also to estimate the Sommerfeld constants (γ) and the Pauli paramagnetic susceptibility (χ) for iron arsenides $BaFe_2As_2$ and $Ba_{0.5}K_{0.5}Fe_2As_2$, assuming the free electron model, as: $\gamma = (\pi^2/3)N(E_F)k_B^2$, and $\chi = \mu_B^2 N(E_F)$. It is seen (Table 2) that both γ and χ increase approximately by 20% as going from $BaFe_2As_2$ to $Ba_{0.5}K_{0.5}Fe_2As_2$.These values are comparable with those obtained for Fe-containing oxypnictides (for example $\gamma = 12.5\,\mathrm{mJ\cdot K^{-2}\cdot mol^{-1}}$ for LaOFeP [26]).

In addition, the calculated Sommerfeld constant γ^{theor} may be useful for simple estimations [27] of the average electron-phonon coupling constant λ (for $BaFe_2As_2$-based SCs, in the assumption of the conventional BCS phonon-mediated mechanism of superconductivity) as $\gamma^{\mathrm{exp}} = \gamma^{\mathrm{theor}}(1+\lambda)$. Within a very crude estimate, using our γ^{theor} for $BaFe_2As_2$ (Table 2) and the measured [20] γ^{exp} ($\sim 16\,\mathrm{mJ/mol\cdot K^2}$) we obtain an empirical value of λ of about 0.5, i.e. these materials should be within the weak coupling limit. For comparison, available experimental and theoretical estimates of λ for other superconducting oxygen-free species with magnetic ions such as $ACNi_3$ anti-perovskites vary from 1.4 to 0.66, see [28].

On the other hand, the superconducting hole-doped iron arsenide $Ba_{0.5}K_{0.5}Fe_2As_2$ is very similar to the above mentioned layered oxypnictides, for which a set of unconventional superconductivity models was proposed, where, for example, pairing interactions might involve magnetic or orbital fluctuations [13–17]. Note that our results indicate that both $Ba_{0.5}K_{0.5}Fe_2As_2$ and $Ba_{0.5}K_{0.5}Fe_2As_2$ are at the border of magnetic instability, and the calculated magnetic moments for their FM states are about $1.90\,\mu_B$/Fe for $BaFe_2As_2$ and about $0.74\,\mu_B$/Fe for $Ba_{0.5}K_{0.5}Fe_2As_2$.

In summary, we studied the electronic structure of the newly discovered 38 K oxygen-free superconductor $Ba_{1-x}K_xFe_2As_2$ in comparison with a parent phase – the tetragonal ternary iron arsenide $BaFe_2As_2$.

The density functional theory predicts that $BaFe_2As_2$ may be described as a *quasi-two-dimensional ionic metal* consisting of insulating Ba sheets and conductive (Fe-As) layers; the bonding between them is ionic, whereas the conduction is strongly anisotropic and happens only in the (Fe-As) layers.

According to our calculations, the density of states at the Fermi level increases by about 20% as a result of hole doping through barium ions substitution. This may be a factor, which favors the occurrence of superconductivity in $Ba_{1-x}K_xFe_2As_2$. On the other hand, this system lies at the border of magnetic instability and, possibly, hole doping suppresses the SDW anomaly to induce superconductivity [23]. Thus, further in-depth studies are necessary to understand possible scenarios of superconducting coupling mechanisms for these systems, which may be of interest as a new material platform for further exploration of the relationships between magnetism and superconductivity for oxygen-free SCs.

1. Y. Kamihara, T. Watanabe, M. Hirano, and H. Hosono, J. Am. Chem. Soc. **130**, 3296 (2008).
2. A. Cho, Science **320**, 433 (2008).
3. H. Takahashi, K. Igawa, K. Arii et al., Nature **453**, 376 (2008).
4. P. Cheng, L. Fang, H. Yang et al., arXiv:0804.0835.
5. G. F. Chen, Z. Li, D. Wu et al., arXiv:0803.3790.
6. X. H. Chen, T. Wu, G. Wu et al., arXiv:0803.3603.
7. Z. A. Ren, J. Yang, W. Lu et al., arXiv:0803.4283.
8. Z. A. Ren, J. Yang, W. Lu et al., arXiv:0803.4234.
9. C. Wang, L. Li, S. Chi et al., arXiv:0804.4290.
10. H.-H. Wen, G. Mu, L. Fang et al., Europhys. Lett. **82**, 17009 (2008).
11. Z. A. Ren, G. C. Che, X. L. Dong, arXiv:0804.2582.
12. V. Johnson and W. Jeitschko, J. Solid State Chem. **11**, 161 (1974).
13. K. Haule, J. H. Shim, and G. Kotliar, arXiv:0803.1279.
14. C. Cao, P. J. Hirschfeld, and H. P. Cheng, arXiv:0803.3236.
15. F. Ma, and Z. Y. Lu, arXiv:0803.3286.
16. G. F. Chen, Z. Li, D. Wu et al., arXiv:0803:4394.
17. A. Nekrasov, Z. V. Pchelkina, and M. V. Sadovskii, JETP Lett. **87**, 647 (2008).
18. E. Z. Kurmaev, R. Wilks, A. Moewes et al., arXiv:0805.0668.
19. A. O. Shorikov, M. A. Korotin, S. V. Streltsov et al., arXiv:0804.3283.
20. M. Rotter, M. Tegel, D. Johrendt et al., arXiv: 0805.4021.
21. M. Pfisterer and G. Nagorsen, Z. Naturforsch. B: Chem. Sci. **35**, 703 (1980).
22. T. Mine, H. Yanagi, T. Kamiya et al., arXiv: 0805.4305.
23. M. Rotter, M. Tegel, and D. Johrendt, arXiv: 0805.4630.
24. P. Blaha, K. Schwarz, G. K. H. Madsen et al., WIEN2k, *An Augmented Plane Wave Plus Local Orbitals Program for Calculating Crystal Properties*, Vienna University of Technology, Vienna, 2001.
25. J. P. Perdew, S. Burke, and M. Ernzerhof, Phys. Rev. Lett. **77**, 3865 (1996).
26. T. M. NcQueen, M. Regulacio, A. J. Williams et al., arXiv:0805.2149.
27. Ch. Walti, E. Felder, C. Degen et al., Phys. Rev. B **64**, 172515 (2001).
28. I. R. Shein and A. L. Ivanovskii, Phys. Rev. B **77**, 104101 (2008).